

**SYNTHESIS, PHYSICOCHEMICAL PROPERTIES AND
PHOTOCATALYTIC ACTIVITY OF ZIRCONIA-TITANIA
HETEROSTRUCTURED NANOCOMPOSITE FOR DEGRADATION OF
PARAQUAT DICHLORIDE**

NUR AFIQAH BINTI BADLI

UNIVERSITI TEKNOLOGI MALAYSIA

**SYNTHESIS, PHYSICOCHEMICAL PROPERTIES AND
PHOTOCATALYTIC ACTIVITY OF ZIRCONIA-TITANIA
HETEROSTRUCTURED NANOCOMPOSITE FOR DEGRADATION OF
PARAQUAT DICHLORIDE**

NUR AFIQAH BINTI BADLI

**A thesis submitted in fulfilment of the
requirements for the award of the degree of
Doctor of Philosophy (Chemistry)**

**Faculty of Science
Universiti Teknologi Malaysia**

MAY 2021

ACKNOWLEDGEMENT

First and foremost, I would like to express my thank you to my respectful supervisor, Dr. Susilawati Toemen whose encouragement, guidance, and support from the initial till final level enabled me to develop an understanding of this research. Her willingness to motivate me contributed tremendously to the project. Next, I would like to thank my co-supervisors, Prof. Dr. Wan Azelee Wan Abu Bakar, Dr. Rusmidah Ali, Dr. Leny Yulianti and Dr. Fazira Ilyana Abdul Razak who have assisted me with their knowledge and involvement throughout my study and research. Their continually and convincingly conveyed a spirit of adventure in regard to research and an excitement in regard to teaching.

I would not forget to thank my beloved family, siblings, and my fellow friends especially Dr. Ernieyanti, Dr. Asmat, Dr. Fatin, Dr. Renu, Dr. Salmiah, Dr. Thana, Afiqah Saadon and Sarina who always accompany me and provide me warm support throughout the whole period. I wish to extend my acknowledgment to past and present Green Chemistry group members for all of their help and support, as well as the entire staff of Faculty of Science especially from Department of Chemistry.

Finally, I wish to extend my gratitude to Universiti Teknologi Malaysia (UTM) for financial support received and the Ministry of Education (MOE) for the award of the MyBrain 15 scholarship granted to me throughout my study.

ABSTRACT

The advanced oxidation process using heterogeneous photocatalyst has been proven as a promising technique for the wide range of organic pollutants degradation in aquatic environment. Paraquat dichloride is a highly toxic organic pollutant that is still being widely used in agricultural sectors. This could cause malicious effects to living things and should be treated immediately. In this study, nanocomposite TiO₂ based photocatalysts incorporated with transition metal oxides were synthesized using modified sol-gel and hydrothermal methods. The photocatalytic activity of the prepared catalysts was examined for the paraquat dichloride degradation in aqueous solution under UV lamp ($\lambda = 365 \text{ nm}$, 12 watts) and fluorescence visible lamp ($\lambda > 400 \text{ nm}$, Philips, 36 watts) for four hours. The photodegradation of paraquat dichloride was monitored using ultraviolet-visible spectrophotometer. The potential catalysts were further accomplished for several optimization studies inclusive of co-catalyst ratio, calcination temperature and catalyst dosage. From the screening results, **ZrO₂/TiO₂ photocatalyst calcined at 750°C was found to give the best photocatalytic activity for both methods.** The characterization analyses showed the presence of crystalline heterostructure ZrTiO₄/Ti₂ZrO₆/TiO₂ species with particle size in the range of 8-25 nm and band gap energy of 3.1 - 3.38 eV. The obtained species were confirmed by X-ray photoelectron spectroscopy and high resolution-transmission electron microscopy. The nano irregular morphology was observed with mesoporous mixtures of Type III and IV isotherms and H2 (b) type hysteresis loop with surface area of 49 m²g⁻¹. The highest photodegradation of 98.45% was obtained using 0.3 g of ZrO₂/TiO₂ (40:60) prepared by hydrothermal method with 100% mineralization after irradiated for four hours. Meanwhile, for sol-gel method, only 84.51% of degradation was obtained over 0.3 g of ZrO₂/TiO₂ (20:80) catalyst. Response surface methodology with Box-Behnken design suggested that 0.3 g of ZrO₂/TiO₂ catalyst with 40:60 Zr to Ti ratio and calcination temperature of 815°C is required to achieve 98.43% of paraquat dichloride degradation. Under this condition, the paraquat dichloride photodegradation achieved 98.87%, higher than the recommended value. Furthermore, the advance optimization on the effect of pH, addition of H₂O₂, sonication treatment, hydrogenation process and immobilization on the support material were also studied but no significant increment was observed for the photodegradation. The suggested active species from the radical scavenger studies were in the order of e⁻ > O₂^{-•} > OH[•] > h⁺. From the mechanistic study, the paraquat cation was adsorbed on the ZrO₂/TiO₂ (40:60) photocatalyst surface while intermediates of monopyridone, C₁₂H₁₆N₂O₄ ion, 4-carboxyl-1-methylpyridium ion were validated by Gaussian 16 software. The mechanism was confirmed following the first-order kinetic in accordance to Langmuir-Hinshelwood model.

ABSTRAK

Proses pengoksidaan termaju menggunakan fotomangkin heterogen telah terbukti sebagai teknik yang menyakinkan bagi degradasi pelbagai pencemar organik di dalam persekitaran akuatik. Paraquat diklorida adalah bahan pencemar organik yang sangat toksik yang masih digunakan secara meluas dalam sektor pertanian. Ia boleh menyebabkan kesan buruk kepada benda hidup dan perlu dirawat dengan segera. Dalam kajian ini, fotopemangkin nanokomposit berasaskan TiO_2 yang digabungkan dengan oksida logam peralihan telah disintesis menggunakan kaedah sol-gel yang diubah suai dan hidroterma. Aktiviti fotopemangkinan mangkin yang disediakan telah diuji bagi degradasi paraquat diklorida di dalam larutan akueus di bawah lampu UV ($\lambda = 365 \text{ nm}$, 12 watt) dan lampu pendarfluor nampak ($\lambda > 400 \text{ nm}$, Philips, 36 watt) selama empat jam. Fotodegradasi paraquat diklorida telah dipantau dengan menggunakan spektrofotometer ultraungu-cahaya nampak. Mangkin yang berpotensi kemudiannya dilengkapi dengan beberapa kajian pengoptimuman termasuk nisbah ko-mangkin, suhu kalsinasi dan dos mangkin. Daripada hasil saringan, $\text{ZrO}_2/\text{TiO}_2$ dikalsin pada 750°C didapati memberikan aktiviti fotomangkinan terbaik bagi kedua-dua kaedah. Hasil analisis pencirian menunjukkan kehadiran struktur hetero berhablur spesies $\text{ZrTiO}_4/\text{Ti}_2\text{ZrO}_6/\text{TiO}_2$ dengan saiz zarah antara 8-25 nm dan tenaga luang jalur 3.1 - 3.8 eV. Spesies yang diperolehi telah disahkan dengan spektroskopi fotoelektron sinar-X dan mikroskopi electron penghantaran resolusi tinggi. Morfologi nano tidak sekata diperhatikan dengan campuran liang meso isoterma jenis III dan IV dan keluk histeresis jenis H2 (b) dengan luas permukaan $49 \text{ m}^2\text{g}^{-1}$. Fotodegradasi tertinggi iaitu 98.45% telah diperolehi menggunakan 0.3 g $\text{ZrO}_2/\text{TiO}_2$ (40:60) yang disediakan melalui kaedah hidroterma dengan pemineralan 100% selepas penyinaran selama empat jam. Sementara itu, bagi kaedah sol-gel, hanya 84.51% degradasi diperolehi menggunakan 0.3 g pemangkin $\text{ZrO}_2/\text{TiO}_2$ (20:80). Kaedah permukaan gerak balas dengan reka bentuk Box-Behnken mencadangkan bahawa 0.3 g mangkin $\text{ZrO}_2/\text{TiO}_2$ dengan nisbah Zr kepada Ti 40:60 dan suhu pengkalsinan 815°C diperlukan untuk mencapai 98.43% degradasi paraquat diklorida. Di bawah keadaan ini, fotodegradasi paraquat diklorida telah mencapai 98.87%, lebih tinggi daripada nilai yang disyorkan. Tambahan pula, pengoptimuman kesan pH, penambahan H_2O_2 , rawatan sonikasi, proses penghidrogenan dan pemegungan pada bahan sokongan juga telah dikaji namun tiada kenaikan ketara fotodegradasi diperhatikan. Spesies aktif yang dicadangkan daripada kajian pemerangkapan radikal adalah mengikut urutan $e^- > \text{O}_2^{\cdot-} > \text{OH}^{\cdot} > \text{h}^+$. Dari kajian mekanistik, kation paraquat telah terjerap pada permukaan fotomangkin $\text{ZrO}_2/\text{TiO}_2$ (40:60) manakala sebatian pertengahan monopiridon, ion $\text{C}_{12}\text{H}_{16}\text{N}_2\text{O}_4$, ion 4-karboksil-1-metilpiridium pula telah disahkan dengan perisian Gaussian 16. Mekanisme telah disahkan mengikuti kinetik kelas pertama sesuai dengan model Langmuir-Hinshelwood.

TABLE OF CONTENTS

	TITLE	PAGE
	DECLARATION	iii
	DEDICATION	iv
	ACKNOWLEDGEMENT	v
	ABSTRACT	vi
	ABSTRAK	vii
	TABLE OF CONTENTS	viii
	LIST OF TABLES	xiii
	LIST OF FIGURES	xv
	LIST OF ABBREVIATIONS AND SYMBOLS	xxi
	LIST OF APPENDICES	xxii
CHAPTER 1	INTRODUCTION	1
1.1	Background of Study	1
1.2	Problem Statements	5
1.3	Objective of Research	6
1.4	Scope of the Research	7
1.5	Significance of the Research	8
CHAPTER 2	LITERATURE REVIEW	11
2.1	Introduction	11
2.2.	Synthesis Methods of TiO ₂ Based Photocatalyst	11
2.2.1	Synthesis of TiO ₂ Based Photocatalyst using Sol-gel Method	12
2.2.2	Synthesis of TiO ₂ Based Photocatalyst using Hydrothermal Method	14
2.3	Optimization and immobilized on the support material	16
2.4	Mechanism of Photocatalytic Degradation	18
2.5	Photocatalytic Degradation of Paraquat dichloride	19

2.6	Photocatalytic Optimization using Response Surface Methodology	22
2.7	Mechanistic Study and the Intermediate products of Paraquat Dichloride	25
CHAPTER 3	EXPERIMENTAL	27
3.1	Introduction	27
3.2	Materials and Chemical	27
3.3	Preparation of Photocatalyst	28
3.3.1	Modified Sol-Gel Method	28
3.3.2	Hydrothermal Method	29
3.4	Photocatalytic Degradation of Paraquat dichloride	30
3.4.1	Preparation of Stock Solution of Paraquat Dichloride	30
3.4.2	Preparation of Standard Calibration Solution	31
3.4.3	Photodegradation Testing	31
3.4.4	Photocatalytic Activity Measurements of Treated Paraquat Dichloride	33
3.4.4.1	Ultraviolet-visible Spectrophotometer (UV-vis)	33
3.4.4.2	Total Organic Carbon (TOC) Measurement)	33
3.5	Characterization of Photocatalyst	34
3.5.1	X-Ray Diffraction (XRD)	34
3.5.2	Field Emission Scanning Electron Microscopy (FESEM) and Energy Dispersive X-Ray (EDX)	35
3.5.3	Transmission Electron Microscopy (TEM)	35
3.5.4	Diffuse Reflectance Ultraviolet-visible (DR UV-vis) Spectroscopy	36
3.5.5	X-ray Photoelectron Spectroscopy (XPS)	36
3.5.6	Nitrogen adsorption-desorption Analysis (NA)	36
3.6	Optimization Parameters	37
3.6.1	Optimization of Photocatalytic Preparation	37
3.6.1.1	Calcination Temperatures	37
3.6.1.2	Co-catalyst Loadings	37

3.6.1.3	Light Source	38
3.6.1.4	Catalyst Dosage	38
3.6.1.5	Response Surface Methodology (RSM)	38
3.6.2.	Reusability of the Potential Catalyst	41
3.6.3	Optimization of Photodegradation Activity	41
3.6.2.1	Initial pH of the Solution	41
3.6.2.2	Addition of Hydrogen peroxide	42
3.6.2.3	Sonication Process	42
3.6.2.4	Hydrogenation process	42
3.6.2.5	Support Materials	43
3.7	Kinetic Study	43
3.8	Mechanistic Study	44
3.8.1	Radical Scavenger Studies	44
3.8.2	Attenuated Total Reflection Fourier Transformed Infrared (ATR-FTIR)	44
3.8.3	High Performance Liquid Chromatography-Mass Spectrometer Quadrupole Time-of-Flight (HP LCMS-QTOF)	45
3.8.4	Structural Confirmation Analysis	45
CHAPTER 4	RESULTS AND DISCUSSION PHOTOCATALYTIC SCREENING, PHYSICOCHEMICAL AND OPTIMIZATION STUDIES OF THE TiO₂ BASED PHOTOCATALYST	47
4.1	Introduction	47
4.2	Photocatalytic Screening of Paraquat Dichloride using Monometallic and Bimetallic photocatalyst	47
4.2.1	Photocatalyst Prepared by the Sol - Gel Method	48
4.2.2	Photocatalyst Prepared by Hydrothermal Method	50
4.3	Physicochemical Studies of the Potential Photocatalyst	53
4.3.1	X-ray Diffraction Spectroscopy (XRD)	53
4.3.2	Field Emission Scanning Electron Microscopy-Energy Dispersion X-ray (FESEM-EDX)	63
4.3.3	Transmission Electron Microscopy (TEM)	72

4.3.4	Diffuse Reflectance UV-vis Spectroscopy	76
4.3.5	X-ray Photoelectron Spectroscopy (XPS)	83
4.3.6	Nitrogen Adsorption/Desorption Analysis	89
4.4	Photocatalytic Activity of Potential ZrO ₂ /TiO ₂ Photocatalyst	97
4.4.1	Effect of Zirconium Loadings	98
4.4.2	Effect of Calcination Temperatures	99
4.4.3	Effect of Co-Catalyst	101
4.4.4	Effect of Photocatalyst Dosage	102
4.5	Reusability Testing over ZrO ₂ /TiO ₂ Photocatalysts	104
4.6	Mineralization Study over ZrO ₂ /TiO ₂ Photocatalysts	105
4.7	Optimization by Response Surface Methodology	106
4.7.1	ZrO ₂ /TiO ₂ Photocatalyst Prepared by Sol-gel Method	106
4.7.2	ZrO ₂ /TiO ₂ Photocatalyst Prepared by Hydrothermal Method	1130
CHAPTER 5	OPTIMIZATION OF REACTION CONDITION FOR PARAQUAT DICHLORIDE DEGRADTION OVER ZrO₂/TiO₂ (40:60) PHOTOCATALYST	121
5.1	Introduction	121
5.2	Effect of Initial pH	121
5.3	Effect of Hydrogen Peroxide	123
5.4	Effect of Sonication Treatment	125
5.5	Effect of Hydrogenation	127
5.6	Effect of Immobilization on the Support	128
CHAPTER 6	MECHANISTIC STUDY	131
6.1	Kinetic Studies on Paraquat dichloride	131
6.2	Mechanistic study	133
6.2.1	Effect of Radical Scavenger Studies	133
6.2.2	HPLC-MS Analysis of Intermediate Product over ZrO ₂ /TiO ₂ (40:60) Photocatalyst	135
6.2.3	FTIR Analysis of Intermediate Product over ZrO ₂ /TiO ₂ (40:60) Photocatalyst	137

6.2.4	Proposed Reaction Pathway of Paraquat Dichloride over ZrO ₂ /TiO ₂ (40:60) Photocatalyst	140
CHAPTER 7	CONCLUSION AND RECOMMENDATIONS	143
7.1	Conclusion	143
7.2	Recommendations	144
REFERENCES		147
APPENDICES		155

LIST OF TABLES

TABLE NO.	TITLE	PAGE
Table 2.1	Intermediate products of Paraquat after irradiation Florencio et al. (2004)	26
Table 3.1	Independent variables and their levels (low, center and high values) for the Box Benhken Design of ZrO ₂ /TiO ₂ photocatalyst prepared by i) Sol-gel, ii) Hydrothermal methods	39
Table 3.2	Experimental matrices for photocatalytic degradation of paraquat degradation using ZrO ₂ /TiO ₂ photocatalyst prepared by sol-gel and hydrothermal methods	40
Table 4.1	Percentage degradation of paraquat dichloride using bimetallic oxide prepared by sol-gel method calcined at different temperatures for 5 hours, [paraquat] = 15 ppm, $\lambda_{UV} = 365 \text{ nm}$, reaction time: 4 hours and catalyst dosage: 0.1 g	50
Table 4.2	Percentage degradation of paraquat dichloride using bimetallic oxide prepared by hydrothermal method calcined at different temperatures for 5 hours, [paraquat] = 15 ppm, $\lambda_{UV} = 365 \text{ nm}$, reaction time: 4 hours and catalyst dosage: 0.1 g	52
Table 4.3	Percentage of anatase to rutile of ZrO ₂ /TiO ₂ photocatalysts at different Zr loadings and calcination temperatures prepared by the sol - gel method	57
Table 4.4	Crystallite size of ZrO ₂ /TiO ₂ photocatalysts at different zirconium loadings and calcination temperatures prepared by sol-gel and hydrothermal methods	62
Table 4.5	Band gap energy of mono TiO ₂ and ZrO ₂ /TiO ₂ photocatalysts at different Zr loadings and calcination temperatures	78
Table 4.6	Binding energies for different types of elements obtained over ZrO ₂ /TiO ₂ photocatalyst prepared by sol-gel method	84
Table 4.7	Binding energy for different types of elements obtained over ZrO ₂ /TiO ₂ photocatalyst prepared hydrothermal method	87

Table 4.8	Texture analysis over ZrO ₂ /TiO ₂ photocatalysts prepared by the sol-gel method at different Zr loadings and calcination temperatures.	89
Table 4.9	Texture analysis over ZrO ₂ /TiO ₂ photocatalysts prepared by the hydrothermal method at different Zr loadings and calcination temperatures.	93
Table 4.10	Percentage degradation of paraquat dichloride using trimetallic oxide prepared by sol-gel method at various co-dopant ratio and calcined at 750°C for 5 hours under UV irradiation, [paraquat] = 15 ppm, λ _{UV} = 365 nm, reaction time: 4 hours and catalyst dosage: 0.1 g	102
Table 4.11	The coded level of the independent variables over ZrO ₂ /TiO ₂ photocatalyst prepared by sol-gel method	108
Table 4.12	ANOVA results of the response surface quadratic model for paraquat degradation over ZrO ₂ /TiO ₂ photocatalyst prepared by sol-gel method	109
Table 4.13	Constraints of each factor for the maximum paraquat degradation over ZrO ₂ /TiO ₂ photocatalyst prepared by sol-gel method	112
Table 4.14	The coded level of the independent variables over ZrO ₂ /TiO ₂ photocatalyst prepared by hydrothermal metho	114
Table 4.15	ANOVA for the response surface quadratic model for paraquat degradation over ZrO ₂ /TiO ₂ photocatalyst prepared by hydrothermal method	116
Table 4.16	Constraints of each factor for the maximum paraquat degradation over ZrO ₂ /TiO ₂ photocatalyst prepared by hydrothermal method	120
Table 6.1	First order of rate constant for the photodegradation of paraquat dichloride , λ _{UV} =365 nm, [paraquat] =15 ppm, reaction time = 4 hours	131
Table 6.2	The intermediate products of paraquat dichloride degradation over ZrO ₂ /TiO ₂ (40:60) photocatalyst	136
Table 6.3	Assignment of the functional group on paraquat dichloride and ZrO ₂ /TiO ₂ (40:60) photocatalyst	138

LIST OF FIGURES

FIGURE NO.	TITLE	PAGE
Figure 1.1	Structure formula of Paraquat dichloride	2
Figure 2.1	Band structure of TiO ₂ -N-x%Zr samples as well as their photocatalytic mechanism	14
Figure 2.2	Band gap positions of TiO ₂ , ZnO and Fe ₂ O ₃	19
Figure 2.3	Schematic representation of photocatalytic reaction mechanism	20
Figure 3.1	Schematic diagram of the home built-photocatalytic reactor	32
Figure 4.1	Percentage degradation of paraquat dichloride using mono TiO ₂ photocatalyst calcined at different temperatures for 5 hours, [paraquat] = 15 ppm, λ _{UV} = 365 nm, reaction time: 4 hours and catalyst dosage: 0.1 g	48
Figure 4.2	Percentage degradation of paraquat dichloride using mono TiO ₂ photocatalyst prepared using the hydrothermal method and was calcined at different temperatures for 5 hours, [paraquat] = 15 p.m., λ _{UV} = 365 nm, reaction time: 4 hours and catalyst dosage: 0.1 g	51
Figure 4.3	XRD diffractograms of mono TiO ₂ prepared using the sol-gel method and was calcined at different calcination temperatures	54
Figure 4.4	XRD diffractograms of ZrO ₂ /TiO ₂ photocatalysts photocatalysts (b) Zoom-in XRD diffractogram patterns of ZrTiO ₄ and ZrTi ₂ O ₆ prepared by the sol-gel method at different Zr loadings and was calcined at 750°C	55
Figure 4.5	XRD diffractograms of ZrO ₂ /TiO ₂ (20:80) photocatalysts photocatalysts (b) Zoom-in XRD diffractogram patterns of ZrTiO ₄ and ZrTi ₂ O ₆ prepared by the sol - gel method at different calcination temperatures	56
Figure 4.6	XRD diffractograms of mono TiO ₂ prepared using the hydrothermal method and was calcined at different calcination temperatures	58
Figure 4.7	XRD diffractograms of ZrO ₂ /TiO ₂ photocatalysts photocatalysts (b) Zoom-in XRD diffractogram patterns of ZrTiO ₄ and ZrTi ₂ O ₆ prepared by hydrothermal method at different zirconium loadings and was calcined at 750°C	59

Figure 4.8	XRD diffractograms of ZrO ₂ /TiO ₂ (40:60) photocatalysts (a) TiO ₂ photocatalysts (b) Zoom-in XRD diffractogram patterns of ZrTiO ₄ and ZrTi ₂ O ₆ prepared by hydrothermal method and was calcined at different calcination temperatures	60
Figure 4.9	FESEM micrographs of a) TiO ₂ photocatalysts calcined at 450°C, (b) 750°C (c) 1000°C and d) ZrO ₂ /TiO ₂ (20:80) photocatalyst calcined at 750°C for 5 hours with a magnification of 25000X prepared by sol-gel method	64
Figure 4.10	FESEM micrographs of photocatalysts (a) ZrO ₂ /TiO ₂ (10:90), (b) ZrO ₂ /TiO ₂ (20:80) and (c) ZrO ₂ /TiO ₂ (30:70) calcined at 750°C and ZrO ₂ /TiO ₂ (20:80) calcined at (d) 700°C and (e) 800°C with magnification of 50000X and was prepared by sol-gel method	65
Figure 4.11	EDX of a) TiO ₂ photocatalysts calcined at 450°C and b) ZrO ₂ /TiO ₂ (20:80) photocatalyst calcined at 750°C for 5 hours prepared by sol-gel method	66
Figure 4.12	EDX mapping profile of a) ZrO ₂ /TiO ₂ (10:90) and b) ZrO ₂ /TiO ₂ (20:80) photocatalysts calcined at 750°C and c) ZrO ₂ /TiO ₂ (20:80) photocatalyst calcined at 800°C for 5 hours prepared by sol-gel method	67
Figure 4.13	FESEM micrographs of mono TiO ₂ photocatalysts calcined at (a) 450°C, (b) 750°C and (c) 1000°C and d) ZrO ₂ /TiO ₂ (40:60) photocatalyst calcined at 750°C for 5 hours with magnification of 25000X prepared by hydrothermal method	68
Figure 4.14	EDX of a) TiO ₂ photocatalysts calcined at 450°C and b) ZrO ₂ /TiO ₂ (20:80) photocatalyst calcined at 750°C for 5 hours prepared by hydrothermal method	69
Figure 4.15	FESEM micrographs of ZrO ₂ /TiO ₂ photocatalysts (a) (30:70), (b) (40:60), (c) (50:50), calcined at 750°C with magnification of 75000X prepared by hydrothermal method	69
Figure 4.16	FESEM micrographs of ZrO ₂ /TiO ₂ (40:60) photocatalyst (a) 700°C, (b) 750°C, (c) 800°C (d) 900°C and 1000°C with magnification of 50000X prepared by hydrothermal method	70
Figure 4.17	EDX mapping profiles a) ZrO ₂ /TiO ₂ (30:70) and b) ZrO ₂ /TiO ₂ (40:60) photocatalysts calcined at 750°C and c) ZrO ₂ /TiO ₂ (40:60) photocatalyst calcined at 700°C prepared by hydrothermal method	72
Figure 4.18	TEM images of a) ZrO ₂ /TiO ₂ (10:90) and b) ZrO ₂ /TiO ₂ (20:80) photocatalysts calcined at 750°C and c) ZrO ₂ /TiO ₂	

	(20:80) photocatalyst calcined at 800°C for 5 hours prepared by sol gel method	73
Figure 4.19	HRTEM images of ZrO ₂ /TiO ₂ (20:80) photocatalyst calcined at 750°C a) TiO ₂ (anatase) b) TiO ₂ (rutile) c) ZrTiO ₄ and d) ZrTi ₂ O ₆ prepared by sol-gel method	74
Figure 4.20	TEM images of a) ZrO ₂ /TiO ₂ (30:70) and b) ZrO ₂ /TiO ₂ (40:60) photocatalysts calcined at 750°C and c) ZrO ₂ /TiO ₂ (40:60) photocatalyst calcined at 700°C prepared by hydrothermal method	75
Figure 4.21	HRTEM image of ZrO ₂ /TiO ₂ (40:60) photocatalyst calcined at 750°C a) TiO ₂ (anatase) b) ZrTi ₂ O ₆ and c) ZrTiO ₄	76
Figure 4.22	a) DR UV diffractograms and b) Tauc plots of mono TiO ₂ photocatalysts calcined at different calcination temperatures and prepared by sol-gel method	77
Figure 4.23	a) DR UV diffractograms and b) Tauc plots of ZrO ₂ /TiO ₂ photocatalysts prepared by sol-gel method at different zirconium loadings and calcination temperatures	79
Figure 4.24	a) DR UV diffractograms and b) Tauc plots of mono TiO ₂ photocatalysts prepared by hydrothermal method and were calcined at different calcination temperatures	80
Figure 4.25	DR UV diffractograms and b) Tauc plots of ZrO ₂ /TiO ₂ photocatalysts prepared by hydrothermal method at different Zr loadings	81
Figure 4.26	a) DR UV diffractograms and b) Tauc plots of ZrO ₂ /TiO ₂ (40:60) photocatalysts prepared by hydrothermal method and were calcined at different calcination temperatures	82
Figure 4.27	XPS spectra of a) ZrO ₂ /TiO ₂ (10:90) and b) ZrO ₂ /TiO ₂ (20:80) calcined at 750°C and c) ZrO ₂ /TiO ₂ (20:80) calcined at 800°C prepared by sol-gel method	83
Figure 4.28	XPS results for different type of elements obtained from a) ZrO ₂ /TiO ₂ (10:90) and b) ZrO ₂ /TiO ₂ (20:80) photocatalyst calcined at 750°C and c) ZrO ₂ /TiO ₂ (20:80) photocatalyst calcined at 800°C prepared by sol-gel method	85
Figure 4.29	XPS spectra of a) ZrO ₂ /TiO ₂ (30:70) photocatalyst calcined at 750°C and ZrO ₂ /TiO ₂ (40:60) calcined at b) 700°C, c) 750°C and d) 800°C prepared by hydrothermal method	86
Figure 4.30	XPS results for different type of elements obtained from of a) ZrO ₂ /TiO ₂ (30:70) calcined at 750°C and ZrO ₂ /TiO ₂	

	(40:60) calcined at b) 700°C, c) 750°C and d) 800°C prepared by hydrothermal method	88
Figure 4.31	Nitrogen adsorption/desorption isotherm plots and pore size distribution of ZrO ₂ /TiO ₂ photocatalysts prepared by sol-gel method at Zr loading of a) 10:90 b) 20:80 and c) 30:70 calcined at 750°C and ZrO ₂ /TiO ₂ (20:80) photocatalysts calcined at d) 700°C and e) 800°C	92
Figure 4.32	Nitrogen adsorption/desorption isotherm plots and pore size distribution of ZrO ₂ /TiO ₂ photocatalysts prepared by hydrothermal method at Zr loading of a) 30:70 b) 40:60 and c) 50:50 calcined at 750°C	94
Figure 4.33	Nitrogen adsorption/desorption isotherm plots and pore size distribution of ZrO ₂ /TiO ₂ (40:60) photocatalyst calcined at a) 700°C b) 800°C c) 900°C and d) 1000°C prepared by hydrothermal method	96
Figure 4.34	Percentage degradation of paraquat dichloride using ZrO ₂ /TiO ₂ photocatalyst prepared by sol-gel method at different zirconium loadings and was calcined at 750°C for 5 hours. [paraquat] = 15 ppm, λ _{UV} = 365 nm, reaction time: 4 hours and catalyst dosage: 0.1 g	97
Figure 4.35	Percentage degradation of paraquat dichloride using ZrO ₂ /TiO ₂ photocatalyst prepared by hydrothermal method at different zirconium loadings and was calcined at 750°C for 5 hours. [paraquat] = 15 ppm, λ _{UV} = 365 nm, reaction time: 4 hours and catalyst dosage: 0.1 g	98
Figure 4.36	Percentage degradation of paraquat dichloride using ZrO ₂ /TiO ₂ (20:80) photocatalyst prepared by sol-gel method and was calcined at different calcination temperatures for 5 hour, [paraquat] = 15 ppm, λ _{UV} = 365 nm, reaction time: 4 hours and catalyst dosage: 0.1 g	100
Figure 4.37	Percentage degradation of paraquat dichloride using ZrO ₂ /TiO ₂ photocatalyst prepared by hydrothermal method and was calcined at different calcination temperatures for 5 hour, [paraquat] = 15 ppm, λ _{UV} = 365 nm, reaction time: 4 hours and catalyst dosage: 0.1 g	101
Figure 4.38	Percentage degradation of paraquat dichloride using ZrO ₂ /TiO ₂ (20:80) and ZrO ₂ /TiO ₂ (40:60) photocatalysts calcined at 750°C for 5 hours with different catalyst dosages, [paraquat] = 15 ppm, λ _{UV} = 365 nm, reaction time: 4 hours	103
Figure 4.39	Reusability testing of ZrO ₂ /TiO ₂ (20:80) and ZrO ₂ /TiO ₂ (40:60) photocatalysts calcined at 750°C for 5 hours, [paraquat] = 15 ppm, λ _{UV} = 365 nm, reaction time: 4 hours and catalyst dosage: 0.3 g	104

Figure 4.40	Percentage mineralization of paraquat dichloride using ZrO_2/TiO_2 photocatalyst calcined at $750^\circ C$ for 5 hours, [paraquat] = 15 pp:m , $\lambda_{UV} = 365$ nm, reaction time: 4 hours, catalyst dosage: 0.3 g	105
Figure 4.41	Fit plot of regression model for paraquat degradation from the experimental design over ZrO_2/TiO_2 photocatalyst prepared by sol-gel method	110
Figure 4.42	3-D surface and contour plots of paraquat degradation as a function of a) calcination temperature and Zr loading, b) calcination temperature and catalyst dosage and c) Zr loading and catalyst dosage over ZrO_2/TiO_2 photocatalyst prepared by sol-gel method	111
Figure 4.43	The predicted and actual values for paraquat degradation over ZrO_2/TiO_2 photocatalyst prepared by hydrothermal method	115
Figure 4.44	(a) 3D and (b) contour plot over effect of calcination temperature and Zr loading on the paraquat degradation with catalyst dosage was kept constant at 0.3 over ZrO_2/TiO_2 photocatalyst prepared by hydrothermal method	117
Figure 4.45	(a) 3D and (b) contour plot over effect of calcination temperature and catalyst dosage on the paraquat degradation with Zr loading was kept constant at 40 wt% over ZrO_2/TiO_2 photocatalyst prepared by hydrothermal method	118
Figure 4.46	(a) 3D and (b) contour plot over effect of Zr loading and catalyst dosage on the paraquat degradation with calcination temperature was kept constant at $850^\circ C$ over ZrO_2/TiO_2 photocatalyst prepared by hydrothermal method	119
Figure 5.1	The effects of initial pH of paraquat dichloride over ZrO_2/TiO_2 (40:60) photocatalyst, [paraquat] = 15 ppm , $\lambda_{UV} = 365$ nm, reaction time: 4 hours and catalyst dosage: 0.3 g	122
Figure 5.2	The effects of different concentrations of hydrogen peroxide on the photocatalytic degradation of paraquat using ZrO_2/TiO_2 (40:60) photocatalyst, [paraquat] = 15 ppm , $\lambda_{UV} = 365$ nm, reaction time: 4 hours and catalyst dosage: 0.3 g	124
Figure 5.3	The effect of sonication treatment over ZrO_2/TiO_2 (40:60) photocatalyst for degradation of paraquat dichloride, [paraquat] = 15 ppm , $\lambda_{UV} = 365$ nm, reaction time: 4 hours and catalyst dosage: 0.3 g	126

Figure 5.4	Percentage degradation of paraquat dichloride using ZrO ₂ /TiO ₂ (40:60) photocatalyst at different temperatures under H ₂ flow for 30 minutes, [paraquat] = 15 ppm, λ _{UV} = 365 nm, reaction time: 4 hours and catalyst dosage: 0.3 g	127
Figure 5.5	Percentage degradation of paraquat dichloride using ZrO ₂ /TiO ₂ (40:60) photocatalyst was calcined at 750°C for 5 hours and was tested at different photocatalyst to PVC ratio, [paraquat] = 15 ppm, λ _{UV} = 365 nm, reaction time: 4 hours and catalyst dosage: 0.3 g	128
Figure 6.1	Kinetic study of paraquat dichloride using ZrO ₂ /TiO ₂ photocatalyst prepared at a) different zirconium loadings calcined at 750°C b) ZrO ₂ /TiO ₂ (40:60) photocatalyst calcined at different calcination temperatures for 5 hours and mono TiO ₂ calcined at 450°C for 5 hours. [paraquat] = 15 ppm, λ _{UV} = 365 nm, reaction time: 4 hours and catalyst dosage: 0.3g	132
Figure 6.2	The radical scavengers studies on the photocatalytic activity of ZrO ₂ /TiO ₂ (40:60) photocatalyst for the degradation of paraquat dichloride, [paraquat] = 15 ppm, λ _{UV} = 365 nm, reaction time: 4 hours and catalyst dosage: 0.3 g	134
Figure 6.3	Chemical structure of the intermediate products	135
Figure 6.4	ATR-FTIR spectra of (a) raw paraquat dichloride and (b) ZrO ₂ /TiO ₂ (40:60) photocatalyst	138
Figure 6.5	FTIR spectrum for determination of adsorbed species on photocatalyst during the photodegradation of paraquat dichloride in aqueous	139
Figure 6.6	Proposed mechanism pathway for photocatalytic degradation of Paraquat in aqueous using ZrO ₂ /TiO ₂ (40:60) photocatalyst under UV irradiation for 4 hours, [paraquat] = 15 ppm, λ _{UV} = 365 nm, catalyst dosage: 0.3 g	141

LIST OF ABBREVIATIONS AND SYMBOL

ANOVA	-	Analysis of Variance
a.u.	-	Arbitrary unit
BBD	-	Box-Behnken design
BE	-	Binding energy
CB	-	Conduction band
CO ₂	-	Carbon dioxide
e-	-	Electron
Eq.	-	Equation
h ⁺	-	Positive hole
H ₂ O ₂	-	Hydrogen peroxide
HCl	-	Hydrochloric acid
hν	-	Photon energy
m/z	-	Mass/charge
PDF	-	Powder diffraction file
rpm	-	Rate per minute
TOC	-	Total organic carbon
UV-Vis	-	Ultraviolet-visible
VB	-	Valence band
W	-	Watt
wt %	-	Weight percentage
zpc	-	Zero point charge
λ	-	Wavelength

LIST OF APPENDICES

APPENDIX	TITLE	PAGE
Appendix A	Conceptual and Operation Research Framework	155
Appendix B	Calculation on the Preparation of Bimetallic Metal Oxide NiO ₂ /TiO ₂ (10:90) Photocatalyst Based on Metal Loading Prepared by Sol-Gel Method	156
Appendix C	List of samples Prepared by Sol-Gel Method	157
Appendix D	Calculation on the Preparation of Bimetallic Metal Oxide NiO ₂ /TiO ₂ (10:90) Photocatalyst Based on Metal Loading Prepared by Hydrothermal Method	158
Appendix E	List of samples prepared by hydrothermal method	159
Appendix F	Standard UV-Vis Calibration Curve for Paraquat Dichloride	160
Appendix G	Control Experiment for Paraquat Dichloride	161
Appendix H	Preparation of Hydrogen Peroxide Stock Solution	162
Appendix I	Peaks Assignment in the X-Ray Diffraction Patterns Mono TiO ₂ and ZrO ₂ /TiO ₂ Photocatalysts Prepared by Sol-Gel Method at Different Calcination Temperatures and Zr Loadings	163
Appendix J	Peaks Assignment in the X-ray Diffraction Patterns of Mono TiO ₂ and ZrO ₂ /TiO ₂ Photocatalysts Prepared by Hydrothermal Method at Different Calcination Temperatures and Zr Loadings	166
Appendix K	Second Order Kinetic Study of Paraquat Dichloride using ZrO ₂ /TiO ₂ Photocatalyst Prepared at a) Different Zirconium Loadings Calcined at 750°C B) ZrO ₂ /TiO ₂ (40:60) Photocatalyst Calcined at Different Calcination Temperatures for 5 Hours and Mono TiO ₂ Calcined at 450°C for 5 Hours	172

Appendix L	LC-MS Chromatograms of Paraquat Dichloride Degradation over ZrO ₂ /TiO ₂ (40:60) Photocatalyst (a) Total Ion Chromatogram (TIC) and (b) Total Compound Chromatogram (TCC)	174
Appendix M	MS Spectra and Peak List of Intermediate Product Identified During the Paraquat Degradation over ZrO ₂ /TiO ₂ Photocatalys	179
Appendix N	Calculation of Structural Stability	182
Appendix O	Publication and Conferences	184

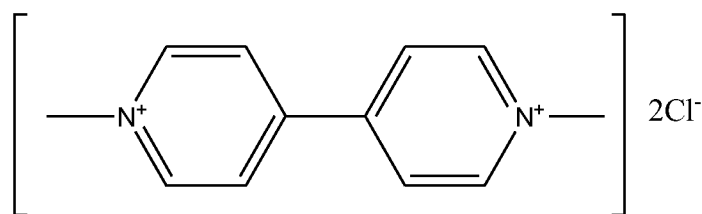
CHAPTER 1

INTRODUCTION

1.1 Background of study

Water is one of the most crucial sources in an ecosystem. About 70 % of the Earth's surface is covered by water. Water pollution has become one of the severe global issues due to the toxic contaminants discharge directly or indirectly from industries or domestic activities without proper treatment. Subsequently causes the consumption of polluted or infected aquatic life and water, resulting in long term illness on the human being. Direct contaminant such as effluent from factories and sewage treatment plants is regulated under the Environmental Quality Act 1974 and Environmental Quality (Sewage and Industrial Effluents) Regulations 1979. Meanwhile, indirect contaminant source is difficult to be identified and this contamination usually comes either from the soil, groundwater and atmosphere via rainwater or agricultural practices like fertilizers and herbicides. These pollutants commonly lead to soil and groundwater contamination leading to ill-associated towards human health and aquatic biodiversity. In common, agricultural residues such as herbicides are strongly adsorbed by soil and may leach into the water bodies by rainfall or runoff which could give a nasty effect on living things mainly for humans.

Recently, the statistic of herbicide usage increased rapidly along with the world population thus increases the food consumption's demand (Diaz Kirmser *et al.*, 2010). Among the herbicide used, paraquat dichloride is one of the active ingredients that was widely used for the agricultural and non-agricultural sectors. This compound is known as methyl viologen with the IUPAC name of 1,1-dimethyl-4,4'-bipyridylium dichloride. The structural formula for paraquat dichloride is shown in Figure 1.1



1, 1'-dimethyl-4, 4'-bipyridinium dichloride

Figure 1.1 Structure formula of Paraquat dichloride

Paraquat dichloride is harmful to humans and could lead to fatal injury if they exceed the lethal dosage. Paraquat poisoning can lead to dysfunctional kidney and liver in humans and animals. Besides that, it also might cause Parkinson's disease (Mandel, Adami and Cole, 2012). However, paraquat dichloride demand increased due to the low-cost and high efficiency to eliminate a wide range of weed made it popular for massive applications. Widespread use of paraquat dichloride application on the soil surface resulted in contamination of water bodies due to heavy rainfall and thus penetrates into the food chain. It also shows high persistence and toxicity in the environment, which has an impact on the environment (Huston and Pignatello, 1999). Hence, it is important to control water contamination to keep the reservoir from being polluted. At present, paraquat dichloride has been banned in certain countries which are Austria, European Union and South Korea (Santos *et al.*, (2013), Cha *et al.*, (2016) and Veríssimo, Bast and Weseler, (2017). Malaysia has also had decided to ban the use of paraquat dichloride starting in January 2020 (The Sun Daily, 2020) but it can be only used for the selected agricultural sector and must be controlled under Pesticide Act 1974.

According to the United States Environmental Protection Agency (2018) the maximum contamination levels (MCL) for paraquat in drinking water is 20 µg/L. While, based on the National Water Quality Standards for Malaysia the maximum concentration level for water resource was set at 10 µg/L (Huang *et al.*, 2012). In Malaysia, the concentration of paraquat dichloride detected is at ranging from 1.49 – 2.29 µg/L (Iguebe and Mohd, (2008), . Ismail, Sameni and Halimah, (2011)). Eventhough the concentration detected still in ppb level but the half-life of paraquat in

the soil can be up to 6 years which might cause a serious impact on humans and other living things in the futures and must be treated (Alexander. M, 1999).

The development in science and technology causes an increase in demand to solve the paraquat dichloride contamination in the aquatic environment. Numerous treatments have been done to overcome these contaminations either by physical, biological or chemical methods. Generally, biological treatment methods such as using enzymes and microorganisms are not effective, because biological methods might produce secondary pollutants after the reaction that need further treatment which will be an additional cost (Han *et al.*, 2009). Besides, some of the organic pollutants are chemically stable and difficult to be degraded by these methods. Moreover, a long retention time is required for the degradation of organic pollution by using biological methods (Wu *et al.*, (2013) and Li *et al.*,(2017)).

The physicochemical method has emerged as a promising method to degraded paraquat dichloride due to its high efficiency and non-toxic properties. Heterogeneous photocatalyst has received considerable attention among researchers. This was due to its effectiveness to degrade and mineralize a wide range of organic and inorganic contaminations in the aquatic environment to harmless by-product(Ahmed *et al.*, 2011). Heterogeneous photocatalytic oxidation is a reaction that involves the use of catalyst that has a different phase from the reactant. Catalyst is a substance that increases the reaction rate by providing an alternate mechanism pathway. Meanwhile, photocatalysis is a process of acceleration of the photoreaction in presence of light. In photogenerated catalysis, the photocatalytic activity depends on the ability of the catalyst to create electron-hole pairs in producing free radicals (hydroxyl radicals, OH•). It will decompose and remove the toxicity of harmful organic chemical substance into carbon dioxide and water (Rauf and Ashraf, 2009).

Among semiconductor material, titanium(IV) dioxide (TiO₂) is the most favourable photocatalyst for heterogenous photocatalysis due to its non-toxicity, the capability of degrading a wide range of pollutants, insoluble in water, good reusability and photostable which makes it a suitable photocatalyst for applications in environmental remediation nowadays (Teh and Mohamed, 2011). Furthermore, an

extensive literature has shown many possibilities of improving the photocatalytic efficiency of TiO₂ especially by incorporating with transition metal oxide. The incorporation of titanium dioxide with transition metal oxide also had received much attention which mostly will contribute to better photocatalytic performance of either using UV irradiation or visible light (Han *et al.*, 2009).

Transition metals exhibit more than one oxidation state that enables to enhance the photocatalytic performance of TiO₂. This was due to ability to act as traps for photogenerated electron and hole pairs as well as charge traps in the lattice of TiO₂. The incorporating with transition metal was believed can prevent the agglomeration of particles thus forming well-defined nanocrystal with high surface area. Moreover, the incorporation of transition metal ions into the matrix could decrease the band-gap energy of TiO₂ and causes a red shift of the absorption edge to the visible-light region. This red shift is caused by the charge-transfer transition between the d electrons of the transition metals and the CB or VB of TiO₂. In addition, transition metal ions in the TiO₂ lattice could delay the recombination rate of photogenerated electron and holes by act as traps thus improving the photocatalytic activity of single TiO₂.

Response surface methodology (RSM) is one of the computational methods that has been used for designing the optimization of the experiment to obtain the optimum response (Sakkas *et al.*, 2010). This technique can be used to develop models from experimental or simulation data and evaluating the individual or interaction between the variables. Among the RSM designs used, Box-Behnken design (BBD) has proven as a useful technique for optimization process as it requires less experimental points with high efficiency (Toemen, Bakar and Ali, (2014) and Tantriratna *et al.*, (2011)). RSM also had been used by researchers in photocatalysis field either for experimental design or for process optimization.

Therefore, the degradation of paraquat dichloride using the photocatalysis method could be the alternative and most effective method. Thus, our current research focus on the synthesis of high efficiency nanocomposite TiO₂ based photocatalyst prepared by sol-gel and hydrothermal methods using transition metal as co-catalyst and immobilized on the support material. In addition, optimization study was carried

out to check the suitability of this technique to optimize the photocatalytic performance of potential photocatalyst over degradation of paraquat dichloride via BBD.

The novelties of this research study are as follows:

- 1) The development of heterostructured $ZrTiO_4/ZrTi_2O_6/TiO_2$ photocatalyst that enhanced the degradation of paraquat dichloride.
- 2) The optimization of the experimental conditions towards the photocatalytic degradation of paraquat dichloride over the potential catalysts using BBD (RSM).
- 3) A proposed cyclic stepwise mechanism for paraquat dichloride degradation under UV irradiation using ZrO_2/TiO_2 (40:60) photocatalyst.
- 4) The new intermediate product for paraquat dichloride degradation and the structural confirmation test using Gaussian 16 software.

1.2 Problem Statements

Paraquat dichloride contamination in the aquatic environment could give dangerous effects on human beings and living things. Therefore, an immediate solution is needed to solve this problem. Although a few treatment methods have been investigated for the degradation of paraquat dichloride however all methods have their drawbacks. Thus in this study, it is proposed to use the photocatalysis technology to degrade paraquat dichloride in solution by using nanocomposite TiO_2 based photocatalyst.

Currently, TiO_2 photocatalyst had gained wide interest in the degradation of various aquatic contaminations. Meanwhile, it is still not suitable for practical application due to its lower photo utilization efficiency and relatively higher band gap (Horváth *et. al.*, 2003, Zu *et. al.*, 2009). However, incorporating with suitable transition metal oxide had shown promising technique to enhanced the efficiency. The incorporation with transition metal oxides will give the useful outcome that might improve the photocatalytic activity. This is due to either the reduction in the band-gap

energy or formation of heterostructured photocatalyst which will increase the generating hydroxyl radicals (OH^\bullet). Besides that, the existence of heterostructure might lead to charge transfer between species thus producing more active species and formation of nanoheterostured had reported could lead to improve the photocatalytic activity even the band gap increases. This was due to cative species existed on the catalyst surface even the band gap energy increases (Li *et al.*, 2016). In addition, only a few studies on the degradation of paraquat dichloride were conducted employing nanocomposite TiO_2 photocatalyst. Furthermore, the synthesis of visible light driven photocatalyst is crucial for a practical use of photocatalysis technique for the degradation of paraquat dichloride in water since artificial UV light is costly and only 11% could be found in the sunlight. In addition, the immobilization of the photocatalyst on the support material also was proven would be useful for industrial application.

In the other hence, the mechanistic study of paraquat dichloride is still vague due to limited research had been conducted using photocatalysis technology especially, using nanocomposite TiO_2 based photocatalyst. Therefore, this study is important to reveals the reaction pathway and the intermediate products formed during the photocatalytic degradation reaction. Thus, giving an insight on effect of the photocatalytic process on surface of the catalyst which can be an added valuable knowledge for the degradation study of paraquat dichloride using photocatalysis process.

1.3 Objective of the research

The objectives of the research are as follow:

1. To synthesize and characterize nanocomposite TiO_2 photocatalyst with transition metal oxides as co-catalyst via modified sol-gel and hydrothermal methods

2. To test and optimize the photocatalytic performance of the prepared photocatalyst for degradation of paraquat dichloride
3. To investigate the kinetic reactions and postulate a mechanism for photodegradation of paraquat dichloride through the analysis on the photocatalyst surface and intermediate products obtained

1.4 Scope of the research

This research was focused on developing a photocatalyst toward the degradation of paraquat dichloride. Therefore, a series of photocatalysts were prepared using TiO₂ as a based catalyst while transition metal oxide was selected as co-catalysts. All single, bimetallic and trimetallic oxide photocatalysts were prepared by sol-gel and hydrothermal methods. The TiO₂ and MO/TiO₂ (MO = NiO, Sc₂O₃, ZrO₂, CoO, CuO, ZnO, MoO₃, RuO, Fe₂O₃, and V₂O₅) photocatalysts were prepared based on the atomic weight percentage.

The photocatalytic performance of the synthesized catalysts was tested under UV irradiation and visible light using a home built a reactor and was monitored by UV-Vis spectrophotometer and total organic carbon (TOC) analysis. The UV lamp ($\lambda = 365\text{nm}$, 12 watts) and compact fluorescence visible lamp ($\lambda > 400\text{ nm}$, Philips, 36 watts) were used as light sources. Then, the best prepared photocatalysts were characterized by using different techniques to study the physicochemical properties which are X-ray diffraction (XRD), field emission scanning electron microscopy-energy dispersion X-ray (FESEM-EDX), transmission electron microscopy (TEM), diffuse reflectance ultraviolet-visible (DR UV-vis) spectroscopy, X-ray photoelectron spectroscopy (XPS) and nitrogen absorption-desorption (NA). Next, the photocatalyst obtained from both methods were optimized on the preparation of photocatalysts using various co-catalysts loading (10:90, 20:80, 30:70, 40:60 and 50:50), calcination temperature (450 - 1000°C) and catalyst dosage (0.1 g to 0.4 g). The reusability testing and mineralization study were carried out using the best catalyst obtained from both methods. Validation

of experimental results was done using response surface methodology (RSM) via Box-Behnken design (BBD).

Then, the best photocatalyst was optimized on the photocatalytic degradation activity. The five studied parameters are initial pH (pH 5,6,7, 8 and 9), hydrogen peroxide concentration (2, 3, 4, 5, 10, 15 and 20 ppm), sonication time (30, 45, and 60 minutes), hydrogenation (700, 750, 800 and 900 °C) and immobilization on PVC and chitosan bead as the supported material using one factor at a time method. Lastly, the mechanistic study was determined by using liquid chromatography-mass spectrometer quadrupole time-of-flight (LCMS-QTOF) and the structural confirmation test was done with Gaussian 16 software to identify the intermediate species and fourier transform infrared spectroscopy-attenuated total reflectance (FTIR-ATR) was used to monitor the adsorbed species on the catalyst surface. The active species was investigated using benzoquinone, ammonium oxalate, silver nitrate and tert-butyl alcohol as scavengers for superoxide radical, holes, electron and hydroxyl radical, respectively.

1.5 Significance of the research

The study gave valuable contributions on the developed preparation method of nanocomposite TiO₂ photocatalyst incorporating with transition metal oxide that have high stability and good photocatalytic performance. The characterizations of the prepared TiO₂-based photocatalyst will provide valuable knowledge on the fundamental requirements for the physicochemical properties of the material prepared either by sol-gel or hydrothermal methods and photocatalytic activities for paraquat dichloride degradation.

This study can be considered as one of the environmentally friendly technologies since photocatalysts are able to degrade harmful pollutants into non-hazardous compounds utilizing light as an energy source. Finally, the success of this

study will contribute to solving water pollution caused by pesticides, especially from the agriculture sector.

REFERENCES

- Abdennouri, M., Baâlala, M., Galadi, A., El Makhfouk, M., Bensitel, M., Nohair, K., Sadiq, M., Boussaoud, A. and Barka, N. (2016). Photocatalytic Degradation of Pesticides by Titanium Dioxide and Titanium Pillared Purified Clays. *Arabian Journal of Chemistry*. 9, S313–S318.
- Adam, F. and Iqbal, A. (2010). The Oxidation of Styrene by Chromium – Silica Heterogeneous Catalyst Prepared From Rice Husk. *Chemical Engineering Journal*. 160(2), 742–750.
- Ahmed, S., Rasul, M.G., Brown, R. and Hashib, M. A (2011). Influence of Parameters on The Heterogeneous Photocatalytic Degradation of Pesticides and Phenolic Contaminants in Wastewater: A Short Review. *Journal of environmental management*. 92(3), 311–30.
- Alexander M. (1999). Biodegradation and Bioremediation, 2nd Edn New York, NY: Academic Press, 45
- Ali, R. and Hassan, S.H. (2008). Degradation Studies on Paraquat and Malathion Using TiO₂/ZnO Based Photocatalyst. *The Malaysian Journal of Analytical Sciences*. 12(1), 77–87.
- Ariffin, M.M. and Anderson, R.A. (2006). LC/MS/MS Analysis of Quaternary Ammonium Drugs and Herbicides in Whole Blood. *Journal of Chromatography B: Analytical Technologies in the Biomedical and Life Sciences*. 842, 91–97.
- Anzures, F.M., Rivas, F.C., Ventura, J.H., Hernández, P.S., Berlier, G. and Zacahua-Tlacuatl, G. (2015). Spectroscopic Characterization of CuO_x/TiO₂-ZrO₂ Catalysts Prepared by a Step Sol-gel Method. *Applied Catalysis A: General*. 489, 218–225.
- Benadji, S., Eloy, P., Leonard, A., Lian, B., Rabia, C. and Gaigneaux, E.M. (2012). Characterization of H³⁺XPMo₁₂-XVXO₄₀ Heteropolyacids Supported on HMS Mesoporous Molecular Sieve and Their Catalytic Performance in Propene Oxidation. *Microporous and Mesoporous Materials*. 154, 153–163.
- Bensaadi, Z., Yeddou-Mezenner, N., Trari, M. and Medjene, F. (2014). Kinetic Studies of B-Blocker Photodegradation on TiO₂. *Journal of Environmental*

Chemical Engineering. 2(3), 1371–1377.

- Bera, S., Lee, J.E., Rawal, S.B. and Lee, W.I. (2016). Size-Dependent Plasmonic Effects of Au And Au@SiO₂ Nanoparticles in Photocatalytic CO₂ Conversion Reaction of Pt/TiO₂. *Applied Catalysis B: Environmental*. 199, 55–63.
- Brigante, M. and Avena, M. (2014). Synthesis, Characterization and Application of a Hexagonal Mesoporous Silica for Pesticide Removal from Aqueous Solution. *Microporous and Mesoporous Materials*. 191, 1–9.
- Cha, E.S., Chang, S. Sen, Gunnell, D., Eddleston, M., Khang, Y.H. and Lee, W.J. (2016). Impact of Paraquat Regulation on Suicide in South Korea. *International Journal of Epidemiology*. 45(2), 470–479.
- Chaibakhsh, N., Ahmadi, N. and Zanjanchi, M.A. (2015). Optimization of Photocatalytic Degradation of Neutral Red Dye using TiO₂ Nanocatalyst via Box-Behnken Design. *Desalination and Water Treatment*. 3994(September), 1–11.
- Chang, S.M. and Doong, R.A. (2006). Characterization of Zr-doped TiO₂ Nanocrystals Prepared by a Nonhydrolytic Sol-Gel Method at High Temperatures. *Journal of Physical Chemistry B*. 110(42), 20808–20814.
- Chen, J., Luo, H., Shi, H., Li, G. and An, T. (2014). Anatase TiO₂ Nanoparticles-Carbon Nanotubes Composite: Optimization Synthesis and The Relationship of Photocatalytic Degradation Activity of Acyclovir in Water. *Applied Catalysis A: General*. 485, 188–195.
- Coleman, N., Perera, S. and Gillan, E.G. (2015). Rapid Solid-State Metathesis Route to Transition-Metal Doped Titanias. *Journal of Solid State Chemistry*. 232, 241–248.
- Colmenares, J.C., Aramendía, M.A., Marinas, A., Marinas, J.M. and Urbano, F.J. (2006). Synthesis, Characterization and Photocatalytic Activity of Different Metal-Doped Titania Systems. *Applied Catalysis A: General*. 306, 120–127.
- Diaz Kirmser, E.M., Mártire, D.O., Gonzalez, M.C. and Rosso, J.A. (2010). Degradation of the Herbicides Clomazone, Paraquat, And Glyphosate by Thermally Activated Peroxydisulfate. *Journal of Agricultural and Food Chemistry*. 58(24), 12858–12862.
- Eleburuike, N.A., Wan Abu Bakar, W.A., Ali, R. and Omar, M.F. (2016). Photocatalytic Degradation of Paraquat Dichloride over CeO₂ -Modified

- TiO₂ Nanotubes And The Optimization Of Parameters By Response Surface Methodology. *RSC Adv.* 6(106), 104082–104093.
- Gao, B., Subagio, D.P. and Lim, T.T.M. (2010). Zr-doped TiO₂ for Enhanced Photocatalytic Degradation of Bisphenol A. *Applied Catalysis A: General.* 375(1), 107–115.
- Ghasemi, S., Rahimnejad, S., Setayesh, S.R., Rohani, S. and Gholami, M.R. (2009). Transition Metal Ions Effect on The Properties and Photocatalytic Activity of Nanocrystalline TiO₂ Prepared in an Ionic Liquid. *Journal of hazardous materials.* 172(2–3), 1573–8.
- Gomathi Devi, L., Girish Kumar, S., Mohan Reddy, K. and Munikrishnappa, C. (2009). Photo Degradation of Methyl Orange an Azo Dye by Advanced Fenton Process using Zero Valent Metallic Iron: Influence of Various Reaction Parameters and its Degradation Mechanism. *Journal of Hazardous Materials.* 164(2–3), 459–467.
- Grillo, R., Clemente, Z., Oliveira, J.L. de, Campos, E.V.R., Chalupe, V.C., Jonsson, C.M., Lima, R. de, Sanches, G., Nishisaka, C.S., Rosa, A.H., Oehlke, K., Greiner, R. and Fraceto, L.F. (2015). Chitosan Nanoparticles Loaded The Herbicide Paraquat: The Influence of The Aquatic Humic Substances on The Colloidal Stability and Toxicity. *Journal of Hazardous Materials.* 286, 562–572.
- Gurin, V. S., Alexeenko, A. A., Kasparov, K. N., and Tyavlovskaya, E. A. (2005). Incorporation of Zirconia and Germania and Ternary Compounds of ZrO₂–GeO₂ into Silica Sol-Gel Matrices. *Materials Science-poland.* 23, 49–60.
- Han, F., Kambala, V.S.R., Srinivasan, M., Rajarathnam, D. and Naidu, R. (2009). Tailored Titanium Dioxide Photocatalysts for the Degradation of Organic Dyes in Wastewater Treatment: A Review. *Applied Catalysis A: General.* 359(1–2), 25–40.
- Hai, H., Wen-jun, X., Jian, Y., Jian-wei. S., Ming-xia. C. and Wen-feng. S. G. (2007). Preparations of TiO₂ Film Coated on Foam Nickel Substrate by Sol-Gel Processes and its Photocatalytic Activity for Degradation of Acetaldehyde. *Journal of Environmental Sciences.* 19(1), 80–85.
- Huston, P.L. and Pignatello, J.J. (1999). Degradation of Selected Pesticide Active Ingredients and Commercial Formulations in Water by The Photo-Assisted Fenton Reaction. *Water Research.* 33(5), 1238–1246.

- Hirano, M. and Ito, T. (2008). Direct Formation of New, Phase-Stable and Photoactive Anatase-Type $Ti_{1-2x}Nb_xSc_xO_2$ Solid Solution Nanoparticles by Hydrothermal Method. *Materials Research Bulletin*. 43(8–9), 2196–2206.
- Hirano, M. and Ito, T. (2011). Effect of Co-Dopant on the Formation and Properties of Anatase-Type Titania Solid Solutions Doped with Niobium. *Journal of Physics and Chemistry of Solids*. 72(6), 661–666.
- Hu, H., Xiao, W. jun, Yuan, J., Shi, J. wei, Chen, M. xia and Shang G, W. Feng (2007). Preparations of TiO_2 Film Coated on Foam Nickel Substrate by Sol-Gel Processes and its Photocatalytic Activity for Degradation of Acetaldehyde. *Journal of Environmental Sciences*. 19(1), 80–85.
- Hirano, M. and Kono, T. (2011). Hydrothermal Synthesis of Rutile-Type Complete Solid Solution Nanoparticles in the TiO_2 - SnO_2 System under Acidic Conditions. *Journal of the American Ceramic Society*. 94(10), 3319–3326.
- Hanaor, D.A.H. and Sorrell, C.C. (2011). Review of the Anatase to Rutile Phase Transformation. *Journal of Materials Science*. 46(4), 855–874.
- Habibi, M. H. and Nasr-Esfahani, M. (2007). Preparation, Characterization and Photocatalytic Activity of a Novel Nanostructure Composite Film Derived from Nanopowder TiO_2 and Sol-gel Process using Organic Dispersant. *Dyes and Pigments*. 75 (3): 714-722.
- Ismail, B.S., Sameni, M. and Halimah, M. (2011). Evaluation of Herbicide Pollution in the Kerian Ricefields of Perak, Malaysia. *Applied Sciences Journal*. 15(1), 05–13.
- Keramati, N., Fallah, N. and Nasernejad, B. (2016). Application of Response Surface Methodology for Optimization of Operational Variables in Photodegradation of Aqueous Styrene Under Visible Light. *Desalination and Water Treatment*. 57(41), 1–9.
- Kim, C.S., Shin, J.W., An, S.H., Jang, H.D. and Kim, T.O. (2012). Photodegradation of Volatile Organic Compounds using Zirconium-Doped TiO_2/SiO_2 Visible Light Photocatalysts. *Chemical Engineering Journal*. 204–205, 40–47.
- Kim, S.W., Khan, R., Kim, T. and Kim, W. (2008). Synthesis, Characterization, and Application of Zr, S Co-doped TiO_2 as Visible-light Active Photocatalyst. *Bull. Korean Chem.* 29(6), 1217–1223.

- Li, W., Bak, T., Atanacio, A. and Nowotny, J. (2016). Photocatalytic Properties of TiO₂: Effect of Niobium and Oxygen Activity on Partial Water Oxidation. *Applied Catalysis B: Environmental*. 198, 243–253.
- Li Y., Ge X. Z., Wang X. Y., Gao R. (2017). The Invention Discloses a Compound Bacterial Agent used to Degrade Paraquat and a Preparation Method. China. Patent No CN 106520618 A. Beijing: National Intellectual Property Administration.
- Lukáč, J., Klementová, M., Bezdička, P., Bakardjieva, S., Šubrt, J., Szatmáry, L., Bastl, Z. and Jirkovský, J. (2007). Influence of Zr as TiO₂ Doping Ion on Photocatalytic Degradation of 4-Chlorophenol. *Applied Catalysis B: Environmental*. 74(1–2), 83–91.
- Mandel, J.S., Adami, H.O. and Cole, P. (2012). Paraquat and Parkinson's Disease: An Overview of the Epidemiology and A Review of Two Recent Studies. *Regulatory Toxicology and Pharmacology*. 62(2), 385–392.
- Mohd, M.A. and Complex, T. (2008). Method of Quantitation For Paraquat Herbicide And Monitoring of Its Levels in Selected Malaysian Rivers. 17, 169–180.
- Merabet, S., Assadi, A.A., Bouzaza, A. and Wolbert, D. (2015). Photocatalytic Degradation of Indole–4-Methylphenol Mixture in an Aqueous Solution: Optimization and Statistical Analysis. *Desalination and Water Treatment*. 3994, 1–12.
- M'Bra, I.C., Atheba, G.P., Robert, D., Drogui, P. and Trokourey, A. (2019). Photocatalytic Degradation of Paraquat Herbicide Using a Fixed Bed Reactor Containing TiO₂ Nanoparticles Coated onto β -SiC Alveolar Foams. *American Journal of Analytical Chemistry*. 10(05), 171–184.
- Misral, H., Sapari, S., Rahman, T., Ibrahim, N., Yamin, B.M. and Hasbullah, S.A. (2018). Evaluation of Novel N-(Dibenzylcarbamothioyl)benzamide Derivatives as Antibacterial Agents by Using DFT and Drug-Likeness Assessment. *Journal of Chemistry*. 2018.
- Ma, W., Jacobs, G., Keogh, R.A., Bukur, D.B. and Davis, B.H. (2012). Applied Catalysis A : General Fischer – Tropsch synthesis : Effect of Pd , Pt , Re , and Ru Noble Metal Promoters on the Activity and Selectivity of a 25% Co/Al₂O₃ Catalyst. *Applied Catalysis A, General*. 437–438, 1–9.

- Nadarajan, R., Wan Abu Bakar, W.A., Ali, R. and Ismail, R. (2015). Photocatalytic Degradation of 1,2-dichlorobenzene using Immobilized TiO₂/SnO₂/WO₃ Photocatalyst under Visible Light: Application of Response Surface Methodology. *Arabian Journal of Chemistry*. 11(1), 34–47.
- Qamar, M., Muneer, M. and Bahnemann, D. (2006). Heterogeneous Photocatalysed Degradation of Two Selected Pesticide Derivatives, Triclopyr and Daminozid in Aqueous Suspensions of Titanium Dioxide. *Journal of Environmental Management*. 80: 99-106.
- Rashad, M.M., Elsayed, E.M., Al-Kotb, M.S. and Shalan, a. E. (2013). The structural, Optical, Magnetic and Photocatalytic Properties of Transition Metal Ions Doped TiO₂ Nanoparticles. *Journal of Alloys and Compounds*. 581, 71–78.
- Rauf, M. a. and Ashraf, S.S. (2009). Fundamental Principles and Application of Heterogeneous Photocatalytic Degradation of Dyes in Solution. *Chemical Engineering Journal*. 151(1–3), 10–18.
- Rao, K. N., Reddy, B. M., Abhishek, B., Seo, Y.-H., Jiang, N. and Park, S.-E. (2009). Effect of Ceria on The Structure and Catalytic Activity of V₂O₅/TiO₂–ZrO₂ For Oxidation of Ethylbenzene to Styrene Utilizing CO₂ as Soft Oxidant. *Applied Catalysis B: Environmental*. 91(3–4), 649–656.
- Sakkas, V., Islam, M. A., Stalikas, C. and Albanis, T. A (2010). Photocatalytic Degradation using Design of Experiments: A Review and Example of The Congo Red Degradation. *Journal of hazardous materials*. 175(1–3), 33–44.
- Santos, M.S.F., Schaule, G., Alves, A. and Madeira, L.M. (2013). Adsorption of Paraquat Herbicide on Deposits From Drinking Water Networks. *Chemical Engineering Journal*. 229, 324–333.
- Shen, Q., Arae, D. and Toyoda, T. (2004). Photosensitization of Nanostructured TiO₂ with CdSe Quantum Dots: Effects of Microstructure and Electron Transport in TiO₂ Substrates. *Journal of Photochemistry and Photobiology A: Chemistry*. 164(1–3), 75–80.
- Su, C.H., Hu, C.C., Sun, Y.C.C. and Hsiao, Y.C. (2016). Highly Active and Thermo-Stable Anatase TiO₂ Photocatalysts Synthesized by A Microwave-Assisted Hydrothermal Method. *Journal of the Taiwan Institute of Chemical Engineers*. 59, 229–236.

- Sun, C., Liu, L., Qi, L., Li, H., Zhang, H., Li, C., Gao, F. and Dong, L. (2011). Efficient Fabrication of ZrO₂-Doped TiO₂ Hollow Nanospheres with Enhanced Photocatalytic Activity of Rhodamine B Degradation. *Journal of Colloid and Interface Science*. 364(2), 288–297.
- Tantriratna, P., Wirojanagud, W., Neramittagapong, S., Wantala, K. and Grisdanurak, N. (2011). Optimization for UV-photocatalytic Degradation of Paraquat over Titanium Dioxide Supported on Rice Husk Silica using Box-Behnken Design. 18, 363–371.
- Teh, C.M. and Mohamed, A.R. (2011). Roles of Titanium Dioxide and Ion-Doped Titanium Dioxide on Photocatalytic Degradation of Organic Pollutants (Phenolic Compounds And Dyes) in Aqueous Solutions: A Review. *Journal of Alloys and Compounds*. 509(5), 1648–1660.
- Toemen, S., Bakar, W.A.W.A. and Ali, R. (2014). Investigation of Ru/Mn/Ce/Al₂O₃ Catalyst for Carbon Dioxide Methanation: Catalytic Optimization, Physicochemical Studies and RSM. *Journal of the Taiwan Institute of Chemical Engineers*. 45(5), 2370–2378.
- Thommes, M., Kaneko, K., Neimark, A. V., Olivier, J.P., Rodriguez-Reinoso, F., Rouquerol, J. and Sing, K.S.W. (2015). Physisorption of Gases, with Special Reference to the Evaluation of Surface Area and Pore Size Distribution (IUPAC Technical Report). *Pure and Applied Chemistry*. 0(0), 1051–1069.
- Veríssimo, G., Bast, A. and Weseler, A.R. (2017). Paraquat Disrupts the Anti-Inflammatory Action of Cortisol in Human Macrophages: In Vitro: Therapeutic Implications for Paraquat Intoxications. *Toxicology Research*. 6(2), 232–241.
- Venkatachalam, N., Palanichamy, M., Arabindoo, B. and Murugesan, V. (2007). Enhanced Photocatalytic Degradation of 4-Chlorophenol by Zr⁴⁺ Doped Nano TiO₂. *Journal of Molecular Catalysis A: Chemical*. 266(1–2), 158–165.
- Wang, S., Zhu, X., Xiong, L., Zhang, Y. and Ren, J. (2016). Toll-like Receptor 4 Knockout Alleviates Paraquat-Induced Cardiomyocyte Contractile Dysfunction Through an Autophagy-Dependent Mechanism. *Toxicology Letters*. 257, 11–22.
- Wan Ngah, W., Endud, C. and Mayanar, R. (2002). Removal of Copper(II) Ions from Aqueous Solution onto Chitosan and Cross-Linked Chitosan Beads. *Reactive and Functional Polymers*. 50(2), 181–190.

- Wu, C.Y., Liu, J.K., Chen, S.S., Deng, X. and Li, Q.F. (2013). Isolation and Characterization of Paraquat-Degrading Extracellular Humus-Reducing Bacteria from Vegetable Field. *Advanced Materials Research*. 807–809, 1026–1030.
- Xu, T., Zhang, L., Cheng, H. and Zhu, Y. (2011). Significantly Enhanced Photocatalytic Performance of ZnO Via Graphene Hybridization and the Mechanism Study. *Applied Catalysis B: Environmental*. 101(3–4), 382–387.
- Yuk Feng Huang, Shin Ying Ang, K.M.L. and T.S.L. (2012). Quality of Water Resources in Malaysia. In *Intech*. p.13.
- Zhang, D. and Zeng, F. (2010). Structural, Photochemical And Photocatalytic Properties of Zirconium Oxide Doped TiO₂ Nanocrystallites. *Applied Surface Science*. 257(3), 867–871.
- Zhu, J., Chen, F., Zhang, J., Chen, H. and Anpo, M. (2006). Fe³⁺-TiO₂ Photocatalysts Prepared by Combining Sol-gel Method with Hydrothermal Treatment and Their Characterization. *Journal of Photochemistry and Photobiology A: Chemistry*. 180(1–2), 196–204.

Appendix O Publications and Conferences

- Nur Afiqah Badli, Rusmidah Ali, Wan Azelee Wan Abu Bakar and Leny Yuliati. Role of Heterojunction $ZrTiO_4/ZrTi_2O_6/TiO_2$ Photocatalyst towards the Degradation of Paraquat Dichloride and Optimization Study by Box–Behnken Design. *Arabian Journal of Chemistry*, 10(2017): 935–943.(I.F 3.298) (Q1).
- Nur Afiqah Badli, Rusmidah Ali and Leny Yuliati. Influence of Zirconium Doped Titanium Oxide towards Photocatalytic Activity of Paraquat. *Advanced Materials Research*, 1107(2015): 377–382. (SCOPUS)
- Nur Afiqah Badli, Rusmidah Ali, Wan Azelee Wan Abu Bakar and Leny Yuliati. Effect of Calcination Temperatures on the Catalytic Activities of Zr-doped Titania (20:80) on the Photodegradation of Paraquat. SKAM 27 Regional Symposium of Malaysian Analytical Chemistry. (2014). - Oral Presenter
- Nur Afiqah Badli, Rusmidah Ali, Wan Azelee Wan Abu Bakar and Leny Yuliati. Photodecomposition Of Paraquat Dichloride Using Zirconium Doped Titania as Catalyst Under UV Irradiation. The 3rd Academic Conference on Natural Science for Master and PhD Students from Asean Countries (CASEAN), Phnom Penh, Cambodia. (2013). - Oral Presenter
- Nur Afiqah Badli, Rusmidah Ali, Wan Azelee Wan Abu Bakar and Leny Yuliati. Influence of Zirconium Doped Titanium Oxide Towards Photocatalytic Activity of Paraquat. 27th Regional Conference on Solid State Science & Technology (RCSST27). (2013). - Oral Presenter
- Nur Afiqah Badli, Rusmidah Ali, Wan Azelee Wan Abu Bakar and Leny Yuliati. Effect of Calcination Temperatures on The Catalytic Activities of Zirconium Doped Titania on The Photodegradation of Paraquat Dichloride 6th International Graduate Conference on Engineering, Science and Humanities (IGCESH 2016). Universiti Teknologi Malaysia, Johor Bahru, Malaysia. (August 2016) -:Oral Presenter